Numerical Simulation of Ice Melting Using the Finite Volume Method

Dr. Mishaal Abdulameer Abdulkareem
Lecturer, Mechanical Engineering Department
College of Engineering, Al-Mustansiriyah University
Baghdad, Iraq
dr.mishal04@gmail.com

ABSTRUCT

The Aim of this paper is to investigate numerically the simulation of ice melting in one and two dimension using the cell-centered finite volume method. The mathematical model is based on the heat conduction equation associated with a fixed grid, latent heat source approach. The fully implicit time scheme is selected to represent the time discretization. The ice conductivity is chosen to be the value of the approximated conductivity at the interface between adjacent ice and water control volumes. The predicted temperature distribution, percentage melt fraction, interface location and its velocity is compared with those obtained from the exact analytical solution. A good agreement is obtained when comparing the numerical results of one dimensional temperature distribution with the analytical results.

KEYWORDS: Finite volume, Stefan problem, moving boundary, phase change, fixed grid.

نمذجة عددية لذوبان الثلج باستخدام طريقة الحجوم المحددة

د. مشعل عبد الأمير عبد الكريم
مدرس في قسم الهندسة الميكانيكية
كلية الهندسة - الجامعة المستنصرية
dr.mishal04@gmail.com

الخلاصة

إن الهدف من هذا البحث هو دراسة النمذجة العددية لذوبان الثلج بشكل أحادي وثنائي البعد باستخدام طريقة cell-centered finite volume method حيث يعتمد النموذج الرياضي على معادلة التوصيل الحراري مع مبدأ الشبكة ثابتة وفرض الحرارة الكامنة كمصدر. تم اختيار نموذج The fully implicit time scheme لتمثل التجزئة الزمنية و تم اختيار معامل التوصيل الحراري للثلج ليمثل القيمة التقريبية للتوصيل الحراري عند الحد الفاصل بين الحجوم المحددة المتجاورة للثلج والماء. تم مقارنة نتائج توزيع درجة الحرارة و النسبة المئوية للمذاب و موقع وسرعة الحد الفاصل مع تلك المتحصلة من الحل الرياضي. تم الحصول على توافق جيد عند مقارنة النتائج العددية لتوزيع درجة الحرارة أحادي البعد مع نتائج الحل الرياضي.

الكلمات الرئيسية: العناصر المحددة، مسألة ستيفان، الحدود المتحركة، تغير الطور، الشبكة الثابتة.

1. INTRODUCTION

The classical Stefan problem is a mathematical model for 'phase-change' or 'moving-boundary' engineering problems involving heat and mass transfer in materials undergoing phase change during thermal processes. Such kind of processes can be the solidification of pure metals, melting of ice, freezing of water and deep freezing of food-stuffs and so on. These materials are assumed to undergo a phase change with a continuously moving liquid-solid isothermal front 'moving boundary' that has to be tracked as part of the solution, (Carslaw and Jaeger, 1959). Owing to the nonlinear form of the thermal energy balance equation at the unknown location of this time-dependent liquid-solid isothermal front 'the phase change constant temperature interface' associated with both, the absorption or release of latent heat and the abrupt discontinuity of properties. Analytical solutions are difficult to obtain except for a limited number of special cases. Therefore, approximate analytical methods are used in the analysis of phase change problems. The Picard's iterative method was used in (Witula et al., 2011). The Lie-Group shooting method was used in (Chein-Shan Liu, 2011). In addition, the heat balance integral method (HBIM) was used in (Myers, 2007). The asymptotic solution for zero-phase type problem for cases having small but finite Biot numbers was used in (Naaktgeboren, 2007). On the other hand, numerical methods are used commonly. The explicit Finite Deference Method was used in (Savovic and Caldwell, 2003). **T**he Faedo-Galerkin Finite Element Method with a Crank-Nicolson time scheme was used in (Rincon and Scardua, 2008). The numerical simulation of ice formation in one and two dimension using the cell-centered Finite Volume Method based on the latent heat source approach was investigated in (Prapainop and Maneeratana, 2004). An enthalpy transforming method with finite volume approach to investigate numerically the steady state natural convection melting process of a two-dimensional square ice cavity was adopted in (Al-Zubaidy, 2006). Several effective modeling techniques with approximate analytical and numerical methods using; Enthalpy Method, Boundary Immobilization Method (BIM), Perturbation Method, Nodal Integral Method and the (HBIM) for the solution of One-Dimensional Stefan problem have been described and compared in (Caldwell and Kwan, 2004). In addition, commercial software packages have been used to solve the 'moving boundary' problem. The melting of snow/ice and the effect of adding salt to the ice/snow has been modeled using MATLAB in (Patrick et al., 2008). The three-dimensional melting of ice around a liquid-carrying tube placed in an adiabatic rectangular cavity was investigated numerically using PHOENICS Code in (Sugawara et al., 2011).

Basically, there are two main approaches for the solution of the Stefan problem. One is the front-tracking method, where the position of the phase boundary is continuously tracked in every time step. Sadoun et al. (2012), has used the Goodman (HBIM) which explicitly tracks the motion of the isothermal liquid-solid front with an explicit finite difference method including modified boundary immobilization scheme in transformed coordinates based on front-tracking and referred to as variable space grid method (VSGM). Hence, this method does not require the discontinuity approximation for isothermal problems and it is poorly suited to multi-dimensional problems due to the difficulties with algorithms of implementations and large computational cost. Zhaochun et al. (2011) presented the moving interface locations and used these location coordinates as the grid points to find out the arrival time of moving interface respectively. Through this approach, the difficulty in mesh generation was avoided completely. Another approach is to use a fixed-grid method, which implicitly contains the moving interface condition within the mathematical model. This method is more flexible than the front-tracking and is suitable for multi-dimensional problems. For the second method, the latent heat is accounted for by either the temperature-based or the enthalpy-based method. The temperature-based approach considers the temperature as the only dependent variable in the governing equation. In order to avoid the discontinuity in isothermal problems, an approximate numerical smoothing must be used and a special integration is needed to compute the latent heat. On the other hand, the enthalpy-based method is further divided into basic enthalpy, apparent heat capacity and latent heat source. In the basic enthalpy scheme, enthalpy is used as the primary variable and the temperature is calculated from a previously defined enthalpy-temperature relation. This method gives reasonably accurate results for metallic solidifying over mushy ranges, but it is complex and computationally expensive and it performs poorly for isothermal problems. In the apparent heat capacity method, the latent heat is calculated from the integration of heat capacity with respect to temperature. As the relationship between heat capacity and temperature in isothermals involves sudden changes, the zero-width phase change interval must be approximated by a narrow range of phase change temperature.

Thus, the size of time step must be small enough that this temperature range is captured in the calculation. In the latent heat source method, the latent heat is included in the source term of the governing differential equation, which is obtained from a prescribed relation between latent enthalpy and temperature.

The aim of this paper is to predict the temperature distribution, the percentage melt fraction, the liquid-solid interface location and its velocity in one and two dimension using the Finite Volume Method based on the fixed grid, latent heat source approach. The fully implicit time scheme is selected to represent the time discretization. The ice conductivity is chosen to be the value of the approximated conductivity at the liquid-solid interface between adjacent ice and water control volumes. To validate the predicted numerical results, it will be compared with those obtained from the exact analytical solution.

2. MATHEMATICAL MODEL

Consider a semi-infinite ice body with $(0 \le x \le \infty)$ is initially at a uniform temperature T_i. This body is suddenly subjected $(at\ x = 0)$ with a constant temperature T_o and $(T_o > T_m > T_i)$ as shown in Fig. (1). It is required to find: The temperature distribution of the solid phase (Ice), T_S and liquid phase (Water), T_L , the Melt fraction, M_r, the Liquid-solid Interface location, $x_m(t)$, and its velocity, $V_{\text{int}erface}$. To solve this classical two-phase Stefan problem, the following assumptions are considered, Ozisik (1993) and Alexiades and Solomon (1993):

1. The thermal properties of solid are not equal to that of liquid.
2. Neglect the volume variation for both phases by assuming a constant and equal density (ρ) for both phases.
3. The thermal properties of a single phase are independent of the temperature.
4. The initial temperature is constant (T_i).
5. A planer and sharp surface (interface) is separating the phases at a constant phase change temperature (T_m) .
6. The Latent heat of fusion (h_{SL}) is constant.
7. Neglect the surface tension and curvature effects at the interface.
8. No convection or radiation heat transfer at the boundaries, only pure and isotropic conduction is considered, and gravity effect is neglected.
9. No internal heat generation.

3. ONE DIMENSIONAL CLOSED FORM SOLUTION

The governing equation with its Initial and Boundary Conditions are:

$$\frac{\partial T_L}{\partial t} = \alpha_L \frac{\partial^2 T_L}{\partial x^2} \qquad for\ (0 \le x \le x_m(t)) \tag{1}$$

$$\frac{\partial T_S}{\partial t} = \alpha_S \frac{\partial^2 T_S}{\partial x^2} \qquad for\ (x_m(t) \le x \le \infty) \tag{2}$$

$$T(x,0) = T_i \tag{3}$$

$$T(0,t) = T_o \tag{4}$$

$$T(\infty,t) = T_i \tag{5}$$

$$T(x_m(t),t) = T_m \tag{6}$$

The energy balance at the interface yields;

$$\left(k_S \frac{\partial T_S}{\partial x}\right)_{x_m(t)} - \left(k_L \frac{\partial T_L}{\partial x}\right)_{x_m(t)} = \rho h_{SL} \frac{dx_m(t)}{dt} \tag{7}$$

Assume: $\delta = \dfrac{x_m(t)}{2\sqrt{\alpha_L t}}$ and $\alpha = \dfrac{\alpha_S}{\alpha_L} = \dfrac{k_S \rho C_L}{k_L \rho C_S}$

The general solution of the temperature distribution for both the liquid and solid phases is given as follows, Carslaw and Jaeger (1959):

$$\frac{T_L(x_L,t) - T_m}{T_o - T_m} = \left[1 - \frac{erf\left(\dfrac{x_L}{2\sqrt{\alpha_L t}}\right)}{erf(\delta)}\right] \tag{8}$$

$$\frac{T_S(x_S,t) - T_i}{T_m - T_i} = \left[\frac{erfc\left(\dfrac{x_S}{2\sqrt{\alpha_S t}}\right)}{erfc\left(\dfrac{\delta}{\sqrt{\alpha}}\right)}\right] \tag{9}$$

Where (δ) is the root of the following transcendental equation:-

$$\frac{1}{erf(\delta)e^{\delta^2}} - \frac{\beta\theta}{erfc\left(\frac{\delta}{\sqrt{\alpha}}\right)e^{\left(\frac{\delta^2}{\alpha}\right)}} = \frac{\delta\sqrt{\pi}}{St} \quad (10)$$

$$(Stefan\ Number)\ St = \frac{Sensible\ heat}{Latent\ heat} = \frac{C_L(T_o - T_m)}{h_{SL}}$$

$$\beta = \sqrt{\frac{k_S \rho C_S}{k_L \rho C_L}} \quad \text{and} \quad \theta = \frac{T_m - T_i}{T_o - T_m}$$

And the interface velocity $(V_{\text{int}erface})$ is as follows;

$$V_{\text{int}erface} = \frac{dx_m(t)}{dt} = \delta\sqrt{\frac{\alpha_L}{t}} \quad (11)$$

And the melt fraction (M_r) is as follows;

$$M_r = \frac{x_m(t)}{L} = \frac{2\delta\sqrt{t\alpha_L}}{L} \quad (12)$$

Where L is a finite length of the domain needed to validate the numerical results of the One-Dimensional model.

4. FINITE VOLUME MODEL

4.1. Grid Generation

In the Finite Volume Method, the first step is to divide the domain into a number of discrete control volumes; (N_x) for One-Dimensional domain and $(N_x N_y)$ for Two-Dimensional domain. A general nodal point is identified by P. In One-Dimensional domain, the nodes to the west and east of P are identified by W and E respectively. The west side boundary of the control volume is referred to by 'w' and the east side of the control volume is referred by 'e', Fig. 2. In Two-Dimensional domain, the nodes to the west, east, south and north of P are identified by W, E, S and N respectively. The side boundaries of the control volume is referred to by; 'w', 'e', 's' and 'n' for the west, east, south and north sides respectively, Fig. 3. The time domain is divided into a number of time steps of size Δt. Variables at the previous time level are indicated by the superscript (o, Old). In contrast, the variables at the new time level are not superscripted, Versteeg and Malalasekera (1995).

4.2. Discretization of One Dimensional Model

A 0.1-m slab has initial temperature $T_i = -5C^o$. The boundary condition at one end of the slab is subjected to a constant temperature $T_o = 20C^o$ while the other end is kept at the value of the initial temperature $T_i = -5C^o$ as illustrated in Fig. 4. Uniform control volumes with size Δx are used. The governing One-Dimensional energy equation is:

$$\rho C\frac{\partial T}{\partial t} = \frac{\partial}{\partial x}\left(k\frac{\partial T}{\partial x}\right) \quad (13)$$

4.2.1. Single Phase Formulation $(T < T_m)$:

$$\frac{\partial H}{\partial t} = \frac{\partial}{\partial t}\left[\int_{T_i}^{T} \rho C_S\, dT\right] \quad (14)$$

Substitute Eq. (14) into Eq. (13), yields;

$$\frac{\partial}{\partial t}\left[\int_{T_i}^{T} \rho C_S\, dT\right] = \frac{\partial}{\partial x}\left(k\frac{\partial T}{\partial x}\right) \quad (15)$$

Multiply Eq. (15) by $(dV.dt), (dV = dx.(1).(1))$ and then integrate over the control volume faces, yields;

$$\int_t^{t+\Delta t}\int_w^e \rho C_S\frac{\partial T}{\partial t}dx.dt = \int_t^{t+\Delta t}\int_w^e \frac{\partial}{\partial x}\left(k\frac{\partial T}{\partial x}\right)dx.dt \quad (16)$$

Using fully implicit scheme;

$$\rho C_S\left(T_P - T_P^o\right)\Delta x = \int_t^{t+\Delta t}\left[\left(k\frac{\partial T}{\partial x}\right)_e - \left(k\frac{\partial T}{\partial x}\right)_w\right]dt \quad (17)$$

4.2.2. Two Phase Formulation $(T \geq T_m)$:

The enthalpy method-latent heat source approach is used to predict the solution of the Two Phase problem, as follows:

$$\frac{\partial H}{\partial t} = \frac{\partial}{\partial t}\left[\int_{T_i}^{T_m} \rho C_S \, dT\right] - \frac{\partial}{\partial t}(\rho h_{SL}) + \frac{\partial}{\partial t}\left[\int_{T_m}^{T} \rho C_L \, dT\right] \quad (18)$$

Substitute Eq. (18) into Eq. (13), yields;

$$\frac{\partial}{\partial t}\left[\int_{T_i}^{T_m} \rho C_S \, dT\right] - \frac{\partial}{\partial t}(\rho h_{SL}) + \frac{\partial}{\partial t}\left[\int_{T_m}^{T} \rho C_L \, dT\right] = \frac{\partial}{\partial x}\left(k \frac{\partial T}{\partial x}\right) \quad (19)$$

Multiply Eq. (19) by $(dV.dt), (dV = dx.(1).(1))$ and then integrate over the control volume faces, yields;

$$\int_t^{t+\Delta t}\int_w^e \rho C_S \frac{\partial T}{\partial t} dx.dt - \int_t^{t+\Delta t}\int_w^e \frac{\partial}{\partial t}(\rho h_{SL}) dx.dt + \int_t^{t+\Delta t}\int_w^e \rho C_L \frac{\partial T}{\partial t} dx.dt = \int_t^{t+\Delta t}\int_w^e \frac{\partial}{\partial x}\left(k \frac{\partial T}{\partial x}\right) dx.dt \quad (20)$$

Using fully implicit scheme;

$$\rho C_S \left(T_P - T_P^o\right)\Delta x - \rho h_{SL} \Delta x + \rho C_L \left(T_P - T_P^o\right)\Delta x = \int_t^{t+\Delta t}\left[\left(k \frac{\partial T}{\partial x}\right)_e - \left(k \frac{\partial T}{\partial x}\right)_w\right] dt \quad (21)$$

Each of the boundary conditions is substituted; into Eq. (17) for discretizing the Single Phase One-Dimensional model and into Eq. (21) for discretizing the Two-Phase One-Dimensional model respectively. Then divide each of the resulting equation by Δt and rearrange yields:

$$a_P T_P = a_E T_E + a_W T_W + a_P^o T_P^o + S_u \quad (22)$$

$$a_P = a_E + a_W + a_P^o - S_P$$

$$\Delta x_w = \Delta x_e = \Delta x = L / N_x$$

Where $\left(a_W, a_E, a_P^o, S_u\right)$ are listed in Table 1.

4.3. Discretization of Two Dimensional Model (Case Study 1)

Consider a $(0.2\cos(\pi/4))m \times (0.2\sin(\pi/4))m$ region of area is initially at a uniform temperature $T_i = -5C^o$. This region is suddenly subjected at the boundaries with a constant temperature $T_o = 20C^o$. Due to summitry, only one-fourth of the total area (shaded area) is modeled as shown in Fig. 5 with no heat flux across the surfaces AD and CD. Uniform control volumes with size Δx and Δy are used. The governing Two-Dimensional energy equation is:

$$\rho C \frac{\partial T}{\partial t} = \frac{\partial}{\partial x}\left(k \frac{\partial T}{\partial x}\right) + \frac{\partial}{\partial y}\left(k \frac{\partial T}{\partial y}\right) \quad (23)$$

4.3.1. Single Phase Formulation $(T < T_m)$:

Substitute Eq. (14) into Eq. (23), yields;

$$\frac{\partial}{\partial t}\left[\int_{T_i}^{T} \rho C_S \, dT\right] = \frac{\partial}{\partial x}\left(k \frac{\partial T}{\partial x}\right) + \frac{\partial}{\partial y}\left(k \frac{\partial T}{\partial y}\right) \quad (24)$$

Multiply Eq. (24) by $(dV.dt), (dV = dx.dy.(1))$ and then integrate over the control volume faces, yields;

$$\int_t^{t+\Delta t}\int_w^e\int_s^n \rho C_S \frac{\partial T}{\partial t} dx.dy.dt = \int_t^{t+\Delta t}\int_s^n\int_w^e \frac{\partial}{\partial x}\left(k \frac{\partial T}{\partial x}\right) dx.dy.dt + \int_t^{t+\Delta t}\int_w^e\int_s^n \frac{\partial}{\partial y}\left(k \frac{\partial T}{\partial y}\right) dx.dy.dt \quad (25)$$

Let $A_x = dy.(1)$, $A_y = dx.(1)$

Using fully implicit scheme;

$$\rho C_S\left(T_P - T_P^o\right)\Delta V = \int_t^{t+\Delta t}\left[\left(kA_x\frac{\partial T}{\partial x}\right)_e - \left(kA_x\frac{\partial T}{\partial x}\right)_w\right]dt + \int_t^{t+\Delta t}\left[\left(kA_y\frac{\partial T}{\partial y}\right)_n - \left(kA_y\frac{\partial T}{\partial y}\right)_s\right]dt \quad (26)$$

4.3.2. Two Phase Formulation $(T \geq T_m)$:

The enthalpy method-latent heat source approach is used to predict the solution of the Two Phase problem, as follows:

Substitute Eq. (18) into Eq. (23), yields;

$$\frac{\partial}{\partial t}\left[\int_{T_i}^{T_m}\rho C_S\,dT\right] - \frac{\partial}{\partial t}\left(\rho h_{SL}\right) + \frac{\partial}{\partial t}\left[\int_{T_m}^{T}\rho C_L\,dT\right] = \frac{\partial}{\partial x}\left(k\frac{\partial T}{\partial x}\right) + \frac{\partial}{\partial y}\left(k\frac{\partial T}{\partial y}\right) \quad (27)$$

Multiply Eq. (27) by $(dV.dt)$, where $(dV = dx.dy)$, and then integrate over the control volume faces, yields;

$$\int_t^{t+\Delta t}\int_w^e\int_s^n \rho C_S\frac{\partial T}{\partial t}dx.dy.dt - \int_t^{t+\Delta t}\int_w^e\int_s^n \frac{\partial}{\partial t}\left(\rho h_{SL}\right)dx.dy.dt + \int_t^{t+\Delta t}\int_w^e\int_s^n \rho C_L\frac{\partial T}{\partial t}dx.dy.dt = \int_t^{t+\Delta t}\int_s^n\int_w^e \frac{\partial}{\partial x}\left(k\frac{\partial T}{\partial x}\right)dx.dy.d + \int_t^{t+\Delta t}\int_w^e\int_s^n \frac{\partial}{\partial y}\left(k\frac{\partial T}{\partial y}\right)dx.dy.dt \quad (28)$$

Using fully implicit scheme;

$$\rho C_S\left(T_P - T_P^o\right)\Delta V - \rho h_{SL}\Delta V + \rho C_L\left(T_P - T_P^o\right)\Delta V = \int_t^{t+\Delta t}\left[\left(kA_x\frac{\partial T}{\partial x}\right)_e - \left(kA_x\frac{\partial T}{\partial x}\right)_w\right]dt + \int_t^{t+\Delta t}\left[\left(kA_y\frac{\partial T}{\partial y}\right)_n - \left(kA_y\frac{\partial T}{\partial y}\right)_s\right]dt \quad (29)$$

Each of the boundary conditions is substituted; into Eq. (26) for discretizing the Single Phase Two-Dimensional model and into Eq. (29) for discretizing the Two-Phase Two-Dimensional model respectively. Then divide each of the resulting equation by Δt and rearrange yields:

$$a_P T_P = a_E T_E + a_W T_W + a_N T_N + a_S T_S + a_P^o T_P^o + S_u \quad (30)$$

$$a_P = a_E + a_W + a_N + a_S + a_P^o - S_P$$

$$\Delta V = \Delta x.\Delta y$$

$$A_x = \Delta y = L_y / N_y$$

$$A_y = \Delta x = L_x / N_x$$

Where $\left(a_W, a_E, a_S, a_N, a_P^o, S_P, S_u\right)$ are listed in Table 2.

4.4. Solver

Equations (22) and (30) are solved using the Tri-Diagonal Matrix Algorithm TDMA, Versteeg and Malalasekera (1995).

5. RESULTS AND DISCUSSION

5.1. One Dimensional Model

The One-Dimensional model with the chosen values of initial and boundary conditions is shown in Fig. 4. Selected material properties for solid and liquid phases are given in Table 3. A constant phase change (Melting) temperature $T_m = 0C^o$. The Latent heat for fusion is constant $h_{SL} = 338\,kJ/kg$. The value of Stefan Number equal (0.25). As the convection of the liquid across cell faces and the induced stress due

to the expansion of the ice are not included in the present work, the density of the ice is approximated to be equal to that of water to ensure the conservation of mass for each control volume.

The first step to validate the numerical solution is to choose the grid and time sizes that are adequate for obtaining the minimum error of results. This task is accomplished through a Gird Independency Test GIT. A grid size of $\Delta x = 1mm$ equivalent to $N_x = 100$ with a time step of $\Delta t = 1\sec$. was obtained with a maximum error of melt fraction of less than 3% as shown in Fig. 6.

Fig. 7 shows a good agreement when the numerical results of temperature distribution is compared with the analytical results at time intervals of $t = 1, 5, 20 \, and \, 40 \min$. using a fully implicit time scheme. The ice conductivity is chosen to be the value of the approximated conductivity at the interface between adjacent ice and water control volumes. The temperature distributions show that ice cells heat up faster due to a high diffusivity $\alpha_S = k_S / \rho C_S$ and a high temperature gradient of almost a linear shape. Once a control volume is melted, its temperature increase will be slow. This clearly illustrates that the rate of heat transfer is predominantly controlled by the position of the melting front as illustrated in Fig. 8 which indicates the percentage of melt fraction as shown in Fig. 9. As ice is a good insulator, the melting front advances at a decelerating rate as shown in Fig. 10.

5.2. Case Study 1:Two Dimensional Model

The Two-Dimensional model with the chosen values of initial and boundary conditions is shown in Fig. 5. Selected material properties for solid and liquid phases are given in Table 3. A constant phase change (Melting) temperature $T_m = 0 C^o$. The Latent heat for fusion is constant $h_{SL} = 338 kJ / kg$. The value of Stefan Number equal (0.25). As the convection of the liquid across cell faces and the induced stress due to the expansion of the ice are not included in the present work, the density of the ice is approximated to be equal to that of water to ensure the conservation of mass for each control volume.

A grid size of $(N_x = 100) \times (N_y = 100)$ are used to model the domain with a time step of $\Delta t = 1\sec$.

To validate the numerical solution of the Two-Dimensional model, the length of the diagonal line BD is assumed to be equal to that of the One-dimensional domain (L=0.1 m). Fig. 11 shows the comparisons between the predicted temperature distribution along the diagonal line BD and the One-Dimensional analytical solution with a fully implicit time scheme and the ice conductivity is chosen to be the value of the approximated conductivity at the interface between adjacent ice and water control volumes at time values of $t = 1, 5, 20 \, and \, 40 \min$. It is clear that the predicted temperature distribution along the diagonal line BD exceeds the One-Dimensional analytical solution due to the area of the exposed corner of the Two-Dimensional domain is approximately twice of that for the One-Dimensional domain. This clearly illustrates that the rate of heat transfer is predominantly controlled by the position of the melting front with a decelerating rate at the beginning of melting process then ending with an accelerated rate due to a decrease in the exposed area of the solid phase of the Two-Dimensional domain, as shown in Fig. 12. The percentage of melt fraction is shown in Fig. 13.

Fig. 14 shows the Two-dimensional temperature distribution of simulation with a fully implicit time scheme and the ice conductivity is chosen to be the value of the approximated conductivity at the interface between adjacent ice and water control volumes at time values of $t = 1, 5, 20 \, and \, 40 \min$. The temperature distribution clearly show heat transfer through both exposed edges, causing a parabolic temperature profile instead of a linear one as in the One-Dimensional temperature distribution.

5.3. Case Study 2:Two Dimensional Model

A Two-Dimensional model of an industrial ice block is simulated with a developed version of the computer program using a body fitted coordinate system. It is subjected to a convection heat transfer boundary condition. Due to summitry, only one-fourth of the total area (shaded area) is modeled as shown in Fig. 15. The value of the free convection heat transfer coefficient between ambient air and outer surface of the ice block is $(h_o = 5 W / m^2 K)$, and the value of the forced convection heat transfer coefficient between the inner surface of the ice block and the flowing fluid is $(h_i = 1500 W / m^2 K)$, Holman (1992). The

ambient air temperature is $\left(T_{\infty} = 20C^{o}\right)$ and the fluid temperature is $\left(T_{f} = 40C^{o}\right)$, (neglecting the pipe thickness effect on temperature). Selected material properties for solid and liquid phases are given in Table 3. A constant phase change (Melting) temperature $T_m = 0C^{O}$. The Latent heat for fusion is constant $h_{SL} = 338\,kJ/kg$. As the induced stress due to the expansion of the ice is not included in the present work, the density of the ice is approximated to be equal to that of water to ensure the conservation of mass for each control volume. A grid size of (20X40) is used to model the domain with a time step of $\Delta t = 1\sec.$ as shown in Fig. 16.

The percentage of melt fraction is shown in Fig. 17.

Fig. 18 shows the Two-dimensional temperature distribution of simulation with a fully implicit time scheme and the ice conductivity is chosen to be the value of the approximated conductivity at the interface between adjacent ice and water control volumes at time values of $t = 2,4,6,8,10\,and\,12\sec.$ The temperature distribution clearly show that ice melting of the Two-Dimensional model (case study 2) is faster than the model of (case study 1).

6. CONCLUSIONS

The modeling of ice melting in one and two dimension using the cell-centered finite volume method of a fully implicit time scheme associated with a fixed grid, latent heat source approach is successfully performed. As the melting front should be of a one control volume thickness, this dominating restriction controls both the time interval and the grid sizes.

The temperature distributions show that ice cells heat up faster with a temperature gradient of almost a linear shape. Once an ice cell is melted, its temperature increase will be slow. This clearly illustrates that the rate of heat transfer is predominantly controlled by the position of the melting front which advances at a decelerating rate at the beginning of melting process then ending with an accelerated rate due to a decrease in the exposed area of the solid phase of the Two-Dimensional domain.

ACKNOWLEDGMENTS

The author would like to thank his wife Dr. Maysoon Basheer Abid (Lecturer at The University of Baghdad, College of Engineering, Water Resources Engineering) for her infinite support and valuable advice.

REFERENCES

Alexiades V. and Solomon A.D., Mathematical Modeling of Melting and Freezing Processes, Hemisphere Publishing Corporation, Washington, 1993.

Al-Zubaidy E.M., "A Computational and instructional study of the effect of natural convection on ice melting", M.Sc. Thesis, Department of Technical Education, University of Technology, Iraq, 2006.

Caldwell J. and Kwan Y.Y., "Numerical methods for one-dimensional Stefan problem", Communications in Numerical Methods in Engineering, Vol. 20, pp. 535-545, John Wiley and Sons, 2004.

Carslaw H.S. and Jaeger J.C., Conduction of Heat in Solids, Oxford University Press, London, UK, 1959.

Chein-Shan Liu, "Solving two typical inverse Stefan problems by using the Lie-Group shooting method", International Journal of Heat and Mass Transfer, Vol. 54, pp. 1941-1949, Elsevier, 2011.

Holman J.P., Heat Transfer, 7th ed in SI Units, McGraw-Hill , UK, 1992.

Myers T.G., Mitchell S.L., Muchatibaya G. and Myers M.Y., "A Cubic heat balance integral method for one-dimensional melting of a finite thickness layer", International journal of Heat and Mass Transfer, Vol. 50, pp.5305-5317, Elsevier, 2007.

Naaktgeboren C., "The zero-phase Stefan problem", International journal of Heat and Mass Transfer, Vol. 50, pp.4614-4622, Elsevier, 2007.

Ozisik M.N., Heat Conduction, John Wiley and Sons, New York, 1993.

Patrick K. et al., "Modeling and simulation of ice/snow melting", the 22nd ECMI Modeling Week Conference, Eindhoven, the Netherlands, 2008.

Prapainop R. and Maneeratana K., "Simulation of ice formation by the finite volume method", Songklanakarin J. Sci. Technol., Vol. 26, No. 1, Jan.-Feb. 2004.

Rincon M.A. and Scardua A., "The Stefan problem with moving boundary", Bol. Soc. Paran. Mat., (3s) V.26, 1-2 , 2008.

Sadoun N., Si-Ahmed E.K. and Legrand J., "On Heat conduction with phase change: accurate explicit numerical method", Journal of Applied Fluid Mechanics, Vol. 5, No. 1, pp- 105-112, 2012.

Savovic S. and Caldwell J., "Finite difference solution of one-dimensional Stefan problem with periodic boundary conditions", International journal of Heat and Mass Transfer, Vol. 46, pp. 2911-2916, Pergamon Press., 2003.

Sugawara M., Komatsu Y. and Beer H., "Three-Dimensional melting of ice around a liquid-carrying tube", Heat Mass Transfer, Vol. 47, pp. 139-145, Springer, 2011.

Versteeg H.K. and Malalasekera W., An Introduction to Computational Fluid Dynamics: The Finite Volume Method, Longman Scientific & Technical, England, 1995.

Witula R., Hetmaniok E., Slota, D. and Zielonka A., "Solution of the two-phase Stefan problem by using the Picards iterative method", Journal of Thermal Science, Vol. 15, Suppl. 1, pp. S21-S26, 2011.

Zhaochun WU, Jianping LUO and Jingmei FENG, "A Noval algorithm for solving the classical Stafan problem", Journal of Thermal Science, Vol. 15, Suppl. 1, pp. S39-S44, 2011.

NOMENCLATURE

A	Cross section area of control volume, m^2
a	Discretization constant
C	Specific heat Capacity, kJ/kg.K
H	Enthalpy, kJ/kg
h	Latent heat of fusion, kJ/kg
k	Thermal conductivity, W/m.K
L	Domain length in the subscripted specified direction, m
M	Melt
N	Number of control volumes in the subscripted specified direction
R	Radius, m
S	Source term constant
St	Stefan number
T	Temperature, C^o
t	Time, second
V	Velocity, m/s, Volume of the control volume element, m^3
x	Distance along the x-direction, m
y	Distance along the y-direction, m

GREEK SYMBOLS

ρ	Density, kg/m^3
δ	Dimensionless melt layer thickness measured from outer surface
θ	Dimensionless ratio of temperature difference
β	Square root of dimensionless ratio of thermal diffusivity

Δ	Step size
α	Thermal diffusivity, m^2/s, Dimensionless ratio of thermal diffusivity
h	Heat transfer coefficient, W/m^2K

SUPERSCRIPTS

o	Old

SUBSCRIPTS

E, e	East
i	Initial
L	Liquid
m	Melt
N, n	North
o	Outer surface
P	Point
r	Ratio
S, s	South
S	Solid
SL	Solid-Liquid
W, w	West

ABREVIATIONS

BIM	Boundary Immobilization Method
GIT	Grid Independency Test
HBIM	Heat Balance Integral Method
TDMA	Tri-Diagonal Matrix Algorithm
VSGM	Variable Space Grid Method

Table 1 Global discretization of one dimensional model.

Phase	a_P^o	**Zone**	a_W	a_E	S_P	S_u
Solid	$\rho C_S \frac{\Delta x}{\Delta t}$	***Internal nodes***	$\frac{k}{\Delta x_w}$	$\frac{k}{\Delta x_e}$	0	0
		West Boundary	0	$\frac{k}{\Delta x_e}$	$-\frac{k}{\Delta x_w/2}$	$\frac{k}{\Delta x_w/2}T_o$
		East Boundary	$\frac{k}{\Delta x_w}$	0	$-\frac{k}{\Delta x_e/2}$	$\frac{k}{\Delta x_e/2}T_i$
Solid + Liquid	$\rho C_S \frac{\Delta x}{\Delta t} + \rho C_L \frac{\Delta x}{\Delta t}$	***Internal nodes***	$\frac{k}{\Delta x_w}$	$\frac{k}{\Delta x_e}$	0	$\rho h_{SL} \Delta x$
		West Boundary	0	$\frac{k}{\Delta x_e}$	$-\frac{k}{\Delta x_w/2}$	$\frac{k}{\Delta x_w/2}T_o + \rho h_{SL} \Delta x$
		East Boundary	$\frac{k}{\Delta x_w}$	0	$-\frac{k}{\Delta x_e/2}$	$\frac{k}{\Delta x_e/2}T_i + \rho h_{SL} \Delta x$

Table 2 Global discretization of two dimensional model (Case Study 1).

Phase	a_P^o	Zone	a_W	a_E	a_N	a_S	S_P	S_u
Solid	$\rho C_S \frac{\Delta V}{\Delta t}$	***Internal nodes***	$\frac{kA_x}{\Delta x_w}$	$\frac{kA_x}{\Delta x_e}$	$\frac{kA_y}{\Delta y_n}$	$\frac{kA_y}{\Delta y_s}$	0	0
		West Boundary (A-B)	0	$\frac{kA_x}{\Delta x_e}$	$\frac{kA_y}{\Delta y_n}$	$\frac{kA_y}{\Delta y_s}$	$-\frac{kA_x}{\Delta x_w/2}$	$\frac{kA_x}{\Delta x_w/2}T_o$
		East Boundary (C-D)	$\frac{kA_x}{\Delta x_w}$	0	$\frac{kA_y}{\Delta y_n}$	$\frac{kA_y}{\Delta y_s}$	0	0
		South Boundary (A-D)	$\frac{kA_x}{\Delta x_w}$	$\frac{kA_x}{\Delta x_e}$	$\frac{kA_y}{\Delta y_n}$	0	0	0
		North Boundary (B-C)	$\frac{kA_x}{\Delta x_w}$	$\frac{kA_x}{\Delta x_e}$	0	$\frac{kA_y}{\Delta y_s}$	$-\frac{kA_y}{\Delta y_n/2}$	$\frac{kA_y}{\Delta y_n/2}T_o$
		Corner A	0	$\frac{kA_x}{\Delta x_e}$	$\frac{kA_y}{\Delta y_n}$	0	$-\frac{kA_x}{\Delta x_w/2}$	$\frac{kA_x}{\Delta x_w/2}T_o$
		Corner B	0	$\frac{kA_x}{\Delta x_e}$	0	$\frac{kA_y}{\Delta y_s}$	$-\frac{kA_x}{\Delta x_w/2}-\frac{kA_y}{\Delta y_n/2}$	$\frac{kA_x}{\Delta x_w/2}T_o+\frac{kA_y}{\Delta y_n/2}T_o$
		Corner C	$\frac{kA_x}{\Delta x_w}$	0	0	$\frac{kA_y}{\Delta y_s}$	$-\frac{kA_y}{\Delta y_n/2}$	$\frac{kA_y}{\Delta y_n/2}T_o$
		Corner D	$\frac{kA_x}{\Delta x_w}$	0	$\frac{kA_y}{\Delta y_n}$	0	0	0
Solid + Liquid	$\rho C_S \frac{\Delta V}{\Delta t} + \rho C_L \frac{\Delta V}{\Delta t}$	***Internal nodes***	$\frac{kA_x}{\Delta x_w}$	$\frac{kA_x}{\Delta x_e}$	$\frac{kA_y}{\Delta y_n}$	$\frac{kA_y}{\Delta y_s}$	0	$\rho h_{SL}\Delta V$
		West Boundary (A-B)	0	$\frac{kA_x}{\Delta x_e}$	$\frac{kA_y}{\Delta y_n}$	$\frac{kA_y}{\Delta y_s}$	$-\frac{kA_x}{\Delta x_w/2}$	$-\frac{kA_x}{\Delta x_w/2}T_o+\rho h_{SL}\Delta V$
		East Boundary (C-D)	$\frac{kA_x}{\Delta x_w}$	0	$\frac{kA_y}{\Delta y_n}$	$\frac{kA_y}{\Delta y_s}$	0	$\rho h_{SL}\Delta V$
		South Boundary (A-D)	$\frac{kA_x}{\Delta x_w}$	$\frac{kA_x}{\Delta x_e}$	$\frac{kA_y}{\Delta y_n}$	0	0	$\rho h_{SL}\Delta V$
		North Boundary (B-C)	$\frac{kA_x}{\Delta x_w}$	$\frac{kA_x}{\Delta x_e}$	0	$\frac{kA_y}{\Delta y_s}$	$-\frac{kA_y}{\Delta y_n/2}$	$\frac{kA_y}{\Delta y_n/2}T_o+\rho h_{SL}\Delta V$
		Corner A	0	$\frac{kA_x}{\Delta x_e}$	$\frac{kA_y}{\Delta y_n}$	0	$-\frac{kA_x}{\Delta x_w/2}$	$\frac{kA_x}{\Delta x_w/2}T_o+\rho h_{SL}\Delta V$
		Corner B	0	$\frac{kA_x}{\Delta x_e}$	0	$\frac{kA_y}{\Delta y_s}$	$-\frac{kA_x}{\Delta x_w/2}-\frac{kA_y}{\Delta y_n/2}$	$\frac{kA_x}{\Delta x_w/2}T_o+\frac{kA_y}{\Delta y_n/2}T_o+\rho h_{SL}\Delta V$
		Corner C	$\frac{kA_x}{\Delta x_w}$	0	0	$\frac{kA_y}{\Delta y_s}$	$-\frac{kA_y}{\Delta y_n/2}$	$\frac{kA_y}{\Delta y_n/2}T_o+\rho h_{SL}\Delta V$
		Corner D	$\frac{kA_x}{\Delta x_w}$	0	$\frac{kA_y}{\Delta y_n}$	0	0	$\rho h_{SL}\Delta V$

Table 3 Thermal properties.

Properties	Solid	Liquid
k (W/m.K)	2.22	0.556
C (kJ/kg.K)	1.762	4.22
$\rho\left(kg/m^3\right)$	1000	1000

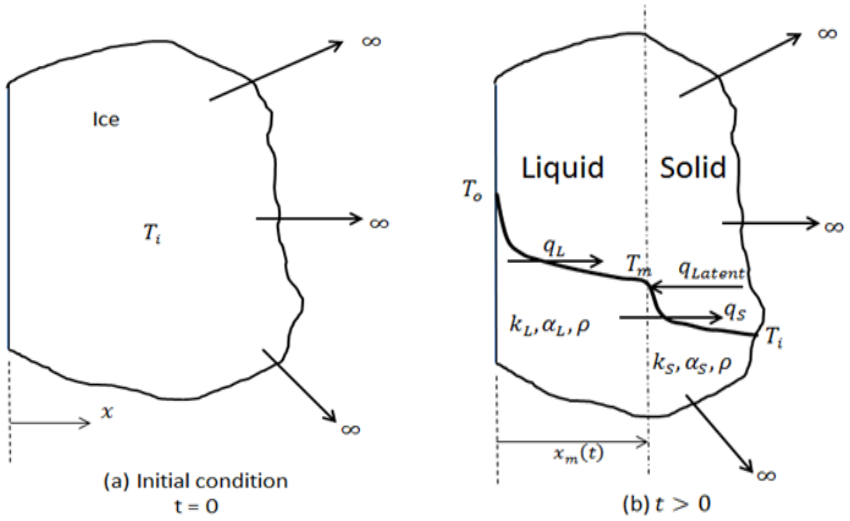

Fig. 1 Mathematical model

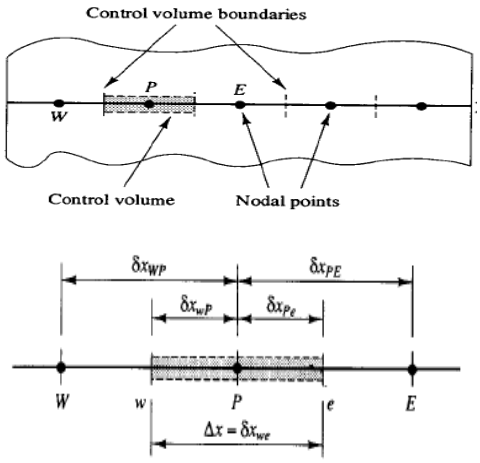

Fig. 2 A typical one dimensional control volume (shaded area)

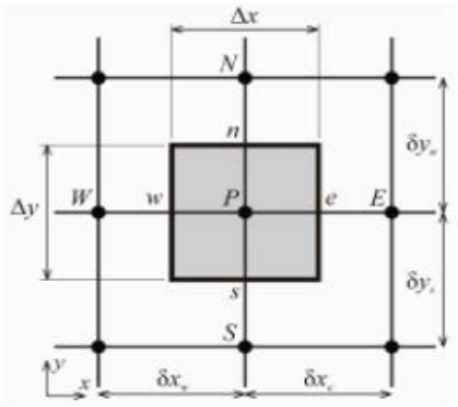

Fig. 3 A typical two dimensional control volume (shaded area).

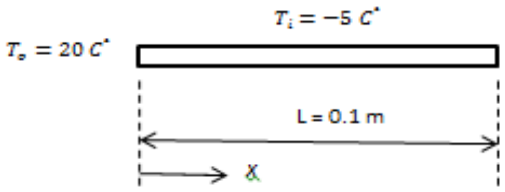

Fig. 4 One dimensional model

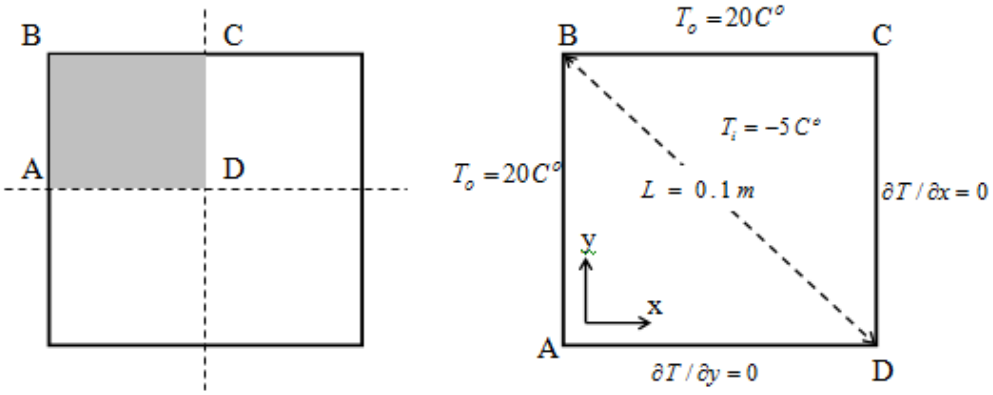

Fig. 5 Case Study 1: Two dimensional model

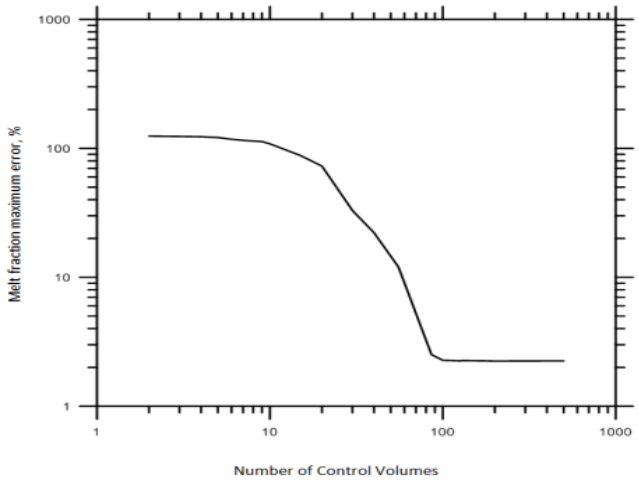

Fig. 6 One dimensional GIT test.

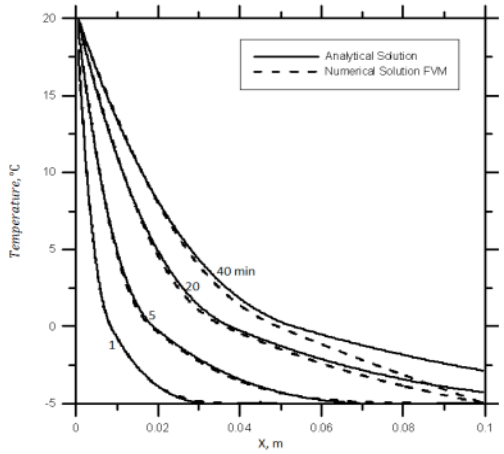

Fig. 7 One dimensional temperature profiles at 1, 5, 20 and 40 min.

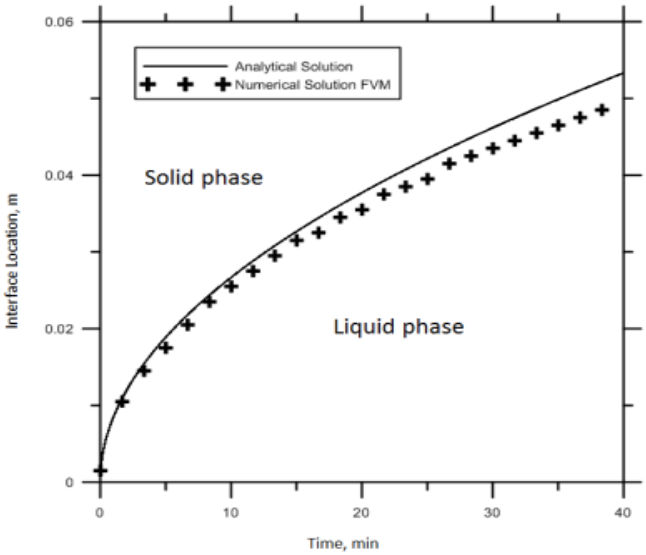

Fig. 8 One dimensional interface location as function of time.

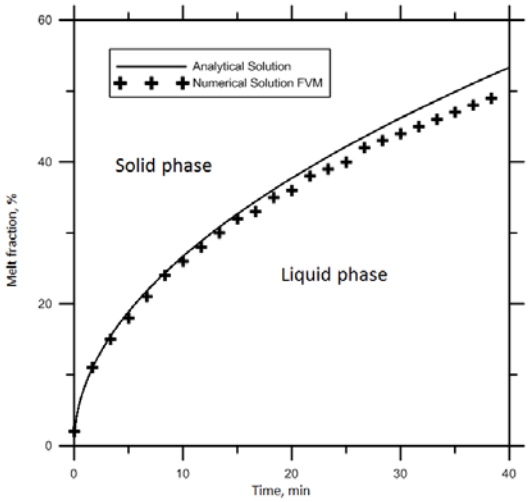

Fig. 9 One dimensional melt fraction as function of time.

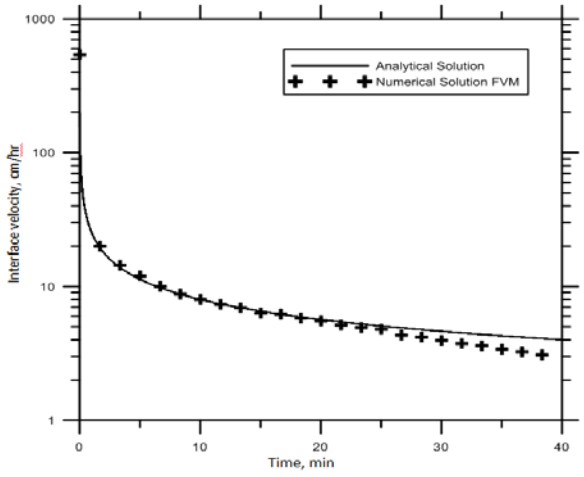

Fig. 10 One dimensional interface velocity as function of time.

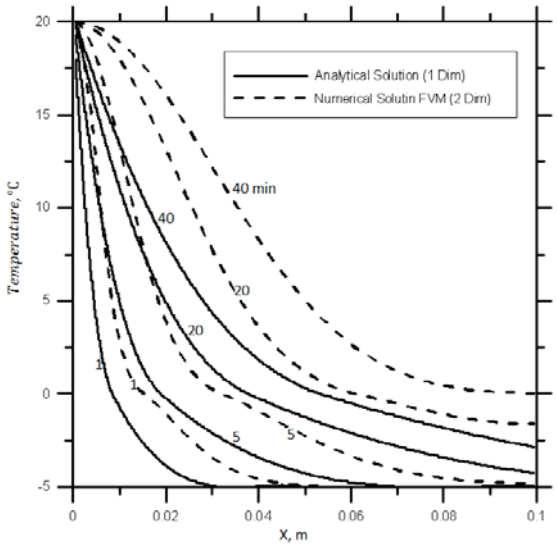

Fig. 11 Predicted temperature profiles (Case Study 1) at the diagonal line BD compared with the one dimensional analytical solution at 1, 5, 20 and 40 min.

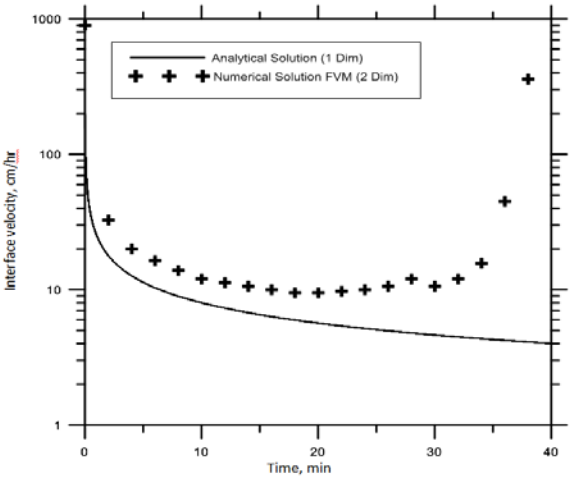

Fig. 12 Predicted velocity (Case Study 1) for a particle at the interface moving along the diagonal line BD compared with the one dimensional analytical solution as function of time.

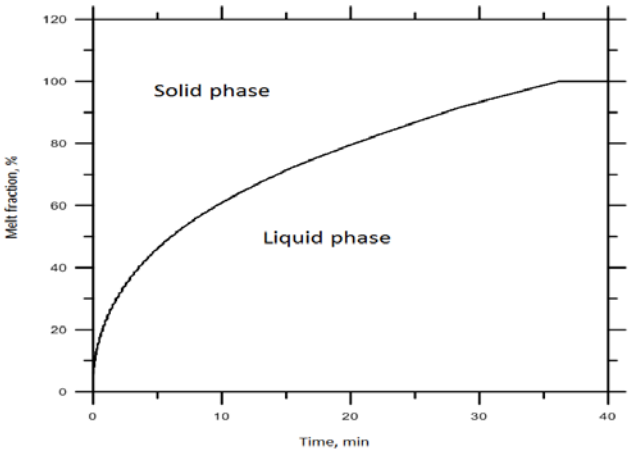

Fig. 13 Case Study 1: Two dimensional melt fraction as function of time.

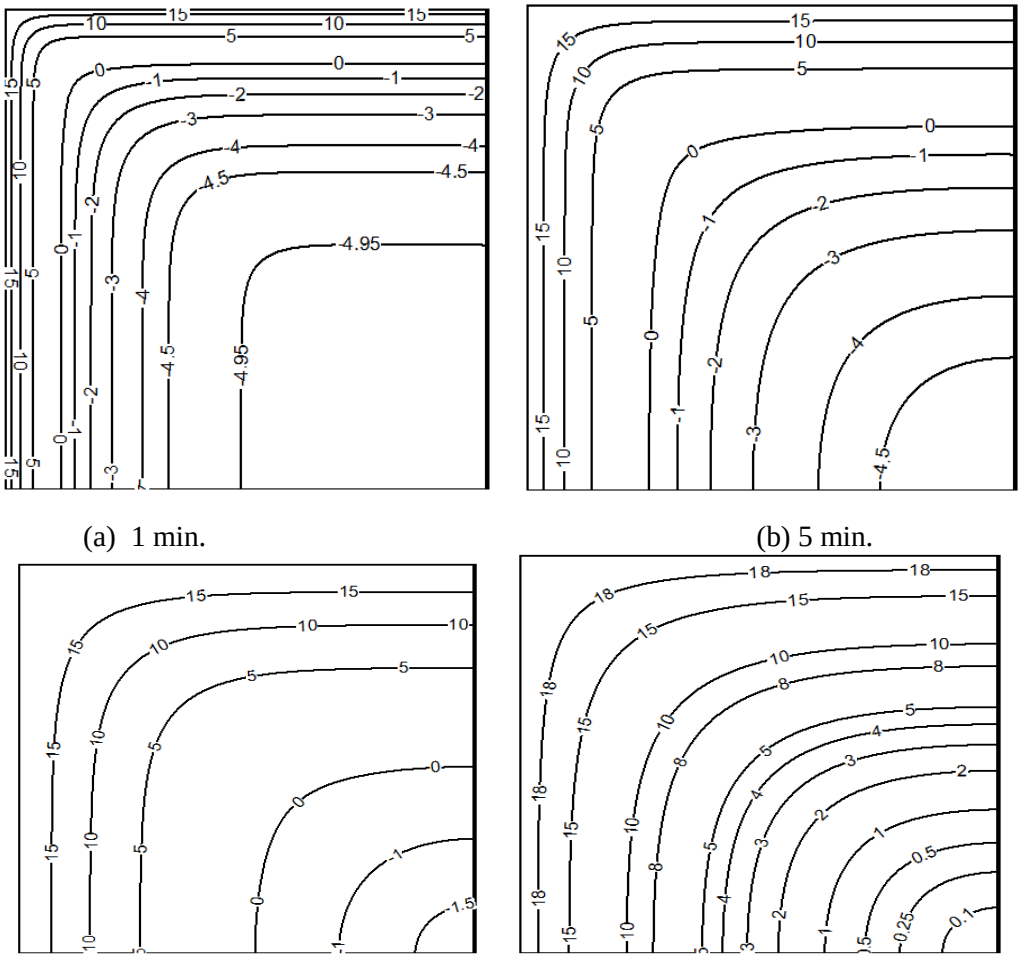

(a) 1 min. (b) 5 min.

(c) 20 min. (d) 40 min.

Fig. 14 Case Study 1: Two dimensional temperature profile.

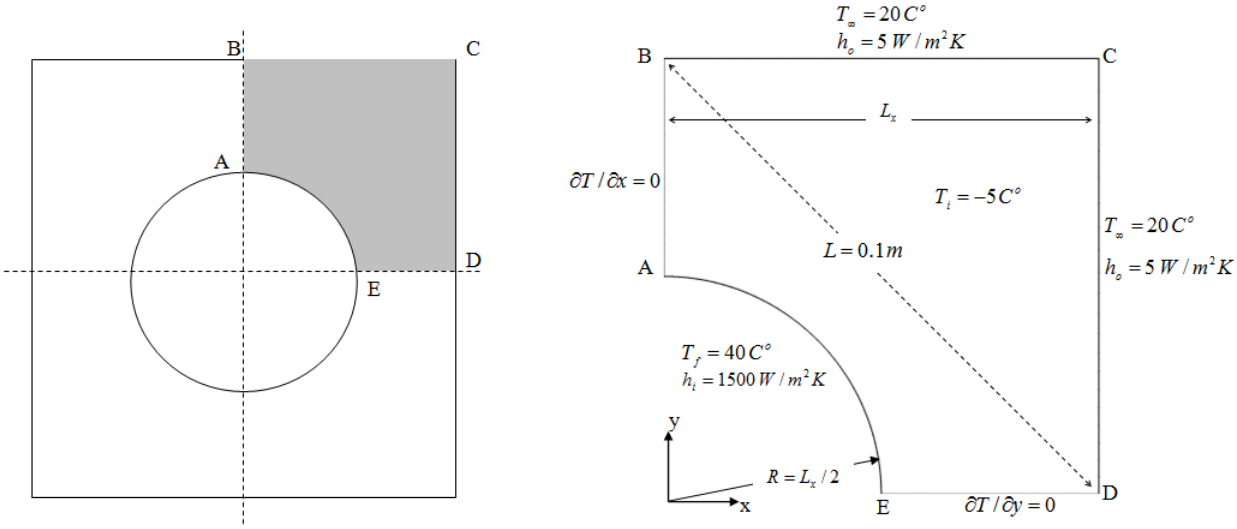

Fig. 15 Case Study 2: Two dimensional model.

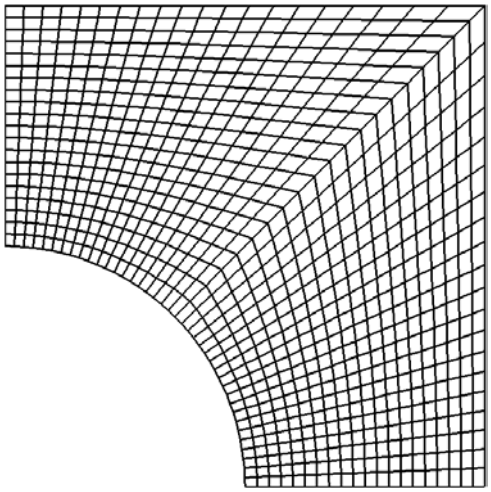

Fig. 16 Case Study 2: Grid Resolution (20X40).

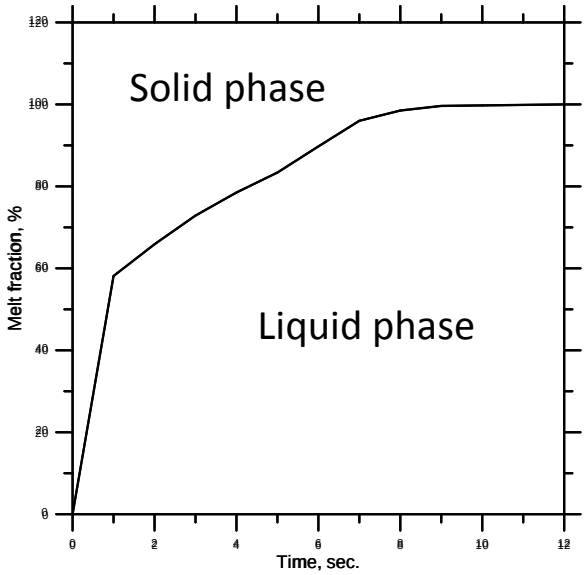

Fig. 17 Case study 2: Two dimensional melt fraction as function of time.

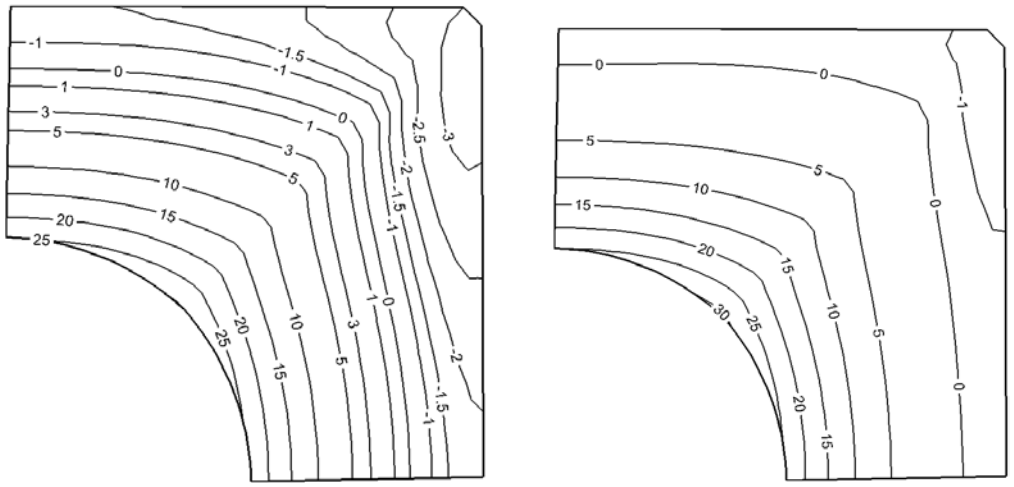

(a) 2 sec. (b) 4 sec.

Fig. 18 Case Study 2: Two dimensional temperature profile.

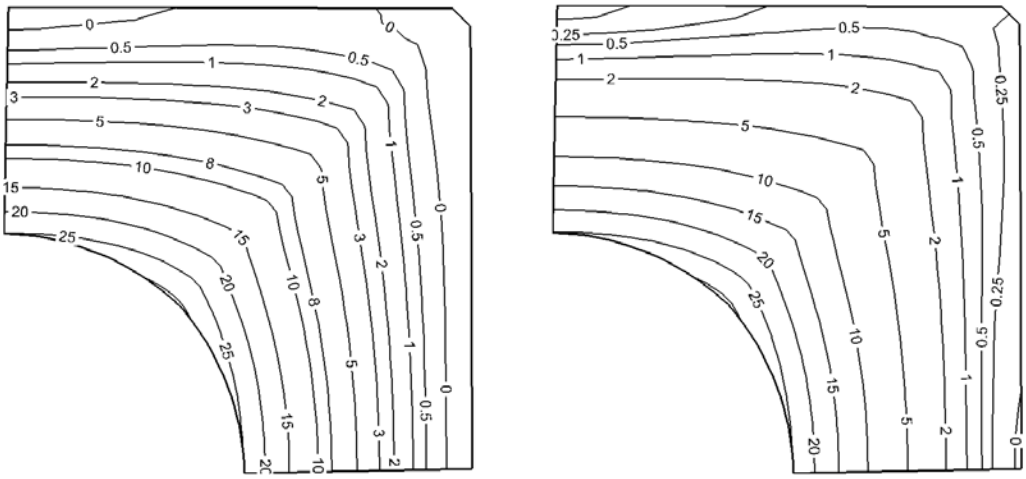

(c) 6 sec. (d) 8 sec.

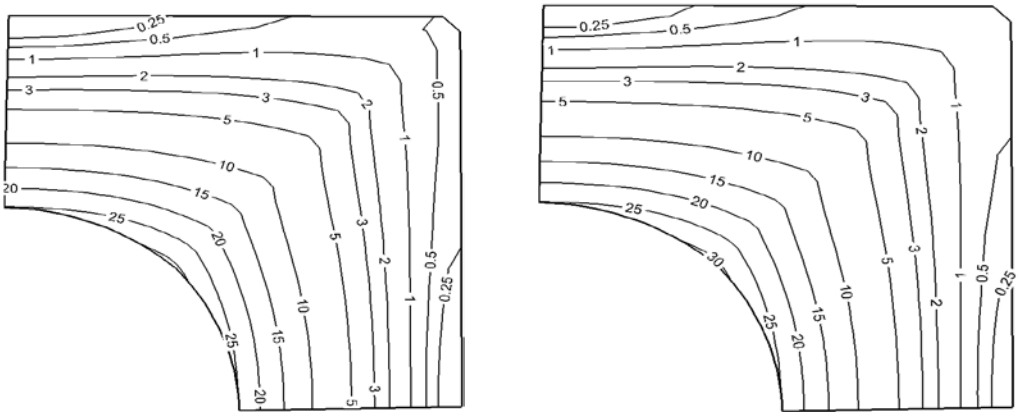

(e) 10 sec. (f) 12 sec.

Fig. 18 Case Study 2: Two dimensional temperature profile.